Assessment of water pollution of waste storage drainage area (a case study in Eskişehir, Türkiye)

Ali KAYABAŞI[1,], Özlem TOYGAR SAĞIN[1,*], Candan GÖKCEOĞLU[2]

[1]Department of Geological Engineering, Faculty of Engineering and Architecture, Eskisehir Osmangazi University, Eskisehir, Türkiye.

[2]Department of Geological Engineering, Faculty of Engineering, Hacettepe University, Ankara, Türkiye.

*Correspondence: toygaro@ogu.edu.tr

ORCIDs:

Ali KAYABAŞI: https://orcid.org/0000-0001-6460-0628

Özlem TOYGAR SAĞIN: https://orcid.org/0000-0002-2516-4250

Candan GÖKÇEOĞLU: https://orcid.org/0000-0003-4762-9933

Abstract: Before 2016, the Eskişehir city landfill was an irregular landfill. Since then, it has been transformed into a regulated landfill. This study aims to investigate the presence of pollution in the landfill drainage area. For this purpose, water samples were collected from the landfill drainage area and the Kadirbey farm spring upstream of the landfill area during the rainy and dry seasons of the year 2021. Analyses of heavy metal content, total Total Dissolved Soil (TDS), Chemical Oxygen Demand (COD), Biochemical Oxygen Demand (BOD), pH, phenol material content, ammonia nitrogen content and conductivity were conducted on the samples. Electrical Resistivity Tomography (ERT) measurements were also performed along the stream bed. According to Turkish Soil Water Quality regulation, the TDS concentrations of all samples, except one, were lower than the limits for 3rd class water quality. The conductivity limits were within the acceptable range for

3rd class water quality. The pH of the water samples was alkaline. The calculated Leachate Pollution Index (LPI) values indicated a pollution risk. The Heavy Metal Pollution Index (HPI) values for the water samples were under 100. Additionally, 75% of the samples fall into the very pure category according to the HEI index, with the remaining samples classified as slightly affected. According to the ERT measurements, soils with low resistivity near the landfill were notably laterally wider. The conductivity decreased with the increasing distance from the landfill site. Low resistivity zones, such as plumes, were disconnected from each other. Shape and volume of highly contaminated plumes decrease towards BH1. Based on the study outcomes, it is recommended to measure the water pollution parameters at periodic intervals within the landfill drainage area.

Key words: Eskişehir**,** ERT, heavy metal pollution, landfill, leachate pollution index

1. Introduction

The global annual municipal soil waste production is approaching 2.2 billion metric tons due to economic development, urbanization, changing lifestyles, and population growth (Çetin et al., 2018; Ucun Ozel et al., 2019; Çetin, 2020; Sevik et al., 2020a, 2020b; Çetin and Jawed, 2021; Koç, 2021; Yucedag et al., 2021; Varol et al., 2022). While developed countries manage their waste with regulated programs, underdeveloped and developing countries often use wild storage methods, which lead to environmental pollution, groundwater contamination, and health problems for the population (Daniel, 1993; Han et al., 2016; Kamaruddin et al., 2017; Sharma et al., 2019). However, efforts to create sanitary landfills continue worldwide to eliminate the negative effects of unregulated landfills, such as landfill sliding, explosions, soil pollution, surface and groundwater pollution, and odor (Baccini et al., 1987; Niininen and Kalliokoski, 1993; Muttamara and Leong, 1997; Çelik et al., 2007). Kumar and Alappad (2005a, b, and c) suggested the Leachate Pollution Index (LPI) as a quantitative method for assessing the leachate pollution material.

Eskişehir sanitary waste storage, once a wild waste landfill area, was rehabilitated and used as a sanitary landfill in 2017 (Ilbank, 2016). The waste deposited in this landfill primarily includes household residues, construction debris, and ash. Additionaly, as of 2017, medical waste has also been hygienically stored at this site.

The current study investigated the potential for water pollution in the area affected by landfill leachate. Two boreholes were drilled to a depth of 30 m. Surface water and groundwater samples were collected during the wet and dry seasons of 2021. Heavy metal content, pH, Total Dissolved Soil (TDS), Chemical Oxygen Demand (COD), Biochemical Oxygen Demand (BOD), Phenolic material concentration, conductivity, and ammonium nitrogen concentration analyses were performed on the surface and groundwater samples. Electrical resistivity tomography (ERT) measurements were taken along the line between the boreholes to determine probable contamination along the Takahasan stream bed in the landfill drainage area. The results obtained from the analyses were discussed in detail concerning contamination.

2. Study area

The study area is located on the border of the Gülpınar neighborhood in the Odunpazarı district of Eskişehir City, Türkiye. The corner coordinates of the area defined in the Universal Transverse Mercator (UTM) projection system Zone 36 is 4,398,000-4,401,000

(Northing) and 288,000–294,000 (Easting). The landfill is near Eskişehir-Seyitgazi D665 State Highway, approximately 7.6 km from the city center of Eskişehir (Figure 1). Settlement areas are located in Gülpınar, approximately 4.2 km east of the landfill; Kayapınar, 6.2 km west; and Sultandere, 9 km west. The Takahasan Stream, which flows seasonally, used to pass through the region before it was converted into a landfill. The bed of the Takahasan Stream was filled in after garbage deposition began. The bed of the Takahasan Stream extends northward for approximately 1.7 km before joining the Ayrıklı Stream, which flows eastward for about 2.5 km and eventually merges with Sarısungur Creek. From there, it continues for an additional distance until it reaches the drying channel of the Eskişehir Waste Water Treatment Plant. Afterward, it continues for about 3 km until it meets the Porsuk River. These streams exhibit a sparse dendritic drainage pattern, with both seasonal and continuous flows directed toward the Porsuk River.

The dominant climate in the region is continental. The maximum temperature was recorded in June (21.7°C), while the minimum temperature was recorded in January (0.1°C) (MGM 2018). Considering the geological perspective, the groundwater and topography map in Figure 2a and a SW-NE oriented geological section in Figure 2b, it is evident that the landfill areas, cemetery areas, Takahasan Stream, and Ayrıklı Stream are situated within deposits of conglomerate, sandstone (Em1), clay, and marl (Em2) from the Eocene-aged Mamuca Formation, Porsuk Formation limestones (Np5), as well as alluvial deposits. Possible faults exist close to both the landfill and the cemetery (Gözler et al., 1985). A groundwater map was prepared by determining the static water levels from 13 wells drilled General Directorate of State Hydraulic Works (Devlet Su Isleri - DSI). As can be seen from Figure 2a, groundwater flows in a northeast (NE) direction

MGM (2018). Turkish State Meteorological Service:https://mgm.gov.tr/eng/forecast-Citiesaspx.

along the Takahasan Stream. Takahasan stream flows during the rainy seasons but is generally dry during other seasons. It merges with its tributaries in the NE direction and is named the Ayrıklı stream. The areas surrounding the Ayrıklı and Takahasan streams are primarily used for agricultural purposes. The highest altitude in the area is 997 m, while the lowest altitude is 806 m.

The Eskişehir landfill area, previously a wild landfill before 2016, was rehabilitated by the Eskişehir municipality (Ilbank 2016) and is now used as a regular landfill storage area. Figure 3 shows views of the wild landfill storage area. The thickness of waste material in the landfill varies between 7 - 37 m. The waste layer in the area was stored irregularly. While the excavation material content was relatively high towards the valley's edges, most domestic waste was observed at the center. First, drainage ditches were excavated at the base of the landfill slopes to discharge the accumulated leachate from the existing landfill body. Perforated drainage pipes were installed, and the leachate water was collected in pools at the pumping station. The landfill was irrigated using return pumps to evaporate some of the leachate in the pools. Regulatory work was carried out in the landfill area, reducing the slopes of the hills and waste were to the minimum possible angle. A balancing layer was applied with a 3% inclination. The landfill rehabilitation was completed by repeating a 50 cm thick drainage layer with geotextile and clay impermeable covers. A reinforced retaining wall, varying in height and approximately 800 meters in length, was constructed to ensure stability (Figure 4a).

31 methane gas collection chimneys were systematically placed in landfills for energy production. The energy production facility was completed in 2017 and commenced the production of electrical energy. The installed capacity of the facility is 11.32 megawatts,

with a current production of 10 megawatts of energy. The Eskişehir integrated facility accepts 800 tons of domestic solid waste daily (Figure 4b and Figure 5).

3. Materials and Methods

3.1. Water and heavy metal analyses

The most important problems in solid waste landfills are the pollution of the surrounding soil, surface water, and groundwater by the leachate generated during the storage of the waste. Leachates are waters containing organic and inorganic pollutants that are likely to interact with the other factors. For this reason, leachate is considered important due to the potential damage it may cause. As a result, landfills pose threats to groundwater, surface water, and soil quality. At a depth of 30 meters, two boreholes (BH1, BH2) were drilled to assess lithological properties and collect groundwater samples. BH1 and BH2 are located 715 meters apart, with BH2 being closer to the waste disposal area. The soil cover was drilled to a depth of 0.5 meters, followed by gravelly, sandy, and silty clay layers extending to depths of 10-15 meters in both boreholes. Beyond this depth, brownish claystone was encountered and drilled down to 30 meters. Average soil compositions for BH1 and BH2 were 9% gravel, 64.5% sand, 17.5% silt, 9% clay and 4% gravel, 49% sand, 30.5% silt, 16.5% clay, respectively. The groundwater levels in the boreholes were measured at one-month intervals.

Groundwater samples were collected from the BH1, BH2, as well as surface water near BH1 and the Kadirbey Farm Spring (KFS). The KFS is located upstream of the landfill site, and therefore, it is not affected by landfill drainage pollution. Water samples were collected on May 13, 2021, during the wet period, and on September 22, 2021, during the dry period in the study area (Table 1).

Water samples were stored in 1-liter polyethylene plastic bottle containers and transferred to the laboratory. Water sample analysis was conducted by the Eskişehir Osmangazi University, Central Research Laboratory Application and Research Center (ARUM), and the Eskişehir Technical University, Environmental Problems Application and Research Center Laboratory (CEVMER). The pH, conductivity, COD, and BOD analysis standards, respectively, are TS EN ISO 10523 (2012), TS 2789+T1 (2011), and SM 2510-B (2021). The samples were collected and preserved following the procedure suggested by TS ISO 5667-10 (2021).

This study used the LPI to calculate leachate pollution, as proposed by Kumar and Alappad (2005a, b, c). The LPI serves as an informational tool for identifying the top priority landfills that may contribute to the environmental pollution (Tamru and Chakma, 2015). The LPI quantifies pollution data between 5 to 100. It consists of three subscripts, such as the inorganic material leachate pollution index (LPI_{inor}), organic material leachate pollution index (LPI_{or}), and heavy metal pollution index (LPI_{hm}). A sum of these subscripts gives the total LPI.

Different indices were proposed in the literature for the evaluation of heavy metal pollution, such as Heavy Metal Pollution Index (HPI) (Horton 1965; Mohan et al. 1996; Prasad and Bose, 2001; Kara et al. 2021), Heavy Metal Evaluation Index (HEI) (Edet and Offiong 2002; Kara et al. 2021). The HPI is used to calculate the contribution of molten metal concentration to the groundwater pollution (Sirajudeen et al., 2014). Rizwan et al. (2011) stated that an HPI value under 100 is safe for human consumption. The HPI is calculated using Eq (1).

$$HPI = \frac{\sum_{i=1}^{n} W_i Q_i}{\sum_{i=1}^{n} W_i} \dots\dots\dots (1)$$

$$Q_i = \sum_{i=1}^{n} \frac{|M_i - L_i|}{S_i - L_i} \dots\dots\dots (2)$$

where M_i is the concentration of the i-th heavy metal, and I_i is the maximum limits of the i-th heavy metal, S_i is the standard permissible concentration value (Mohan et al. 1996). Q_i is sub-index of the i-th parameter, W_i is the unit weight of the i-th parameter, and n is the number of parameters considered.

The HEI, also known as Metal Index (Edet and Offiong 2002; Tamasi and Cini, 2003), assesses the heavy metal risk in water concentration. It is computed using Eq. (3);

$$HEI = \sum_{i=1}^{n} \frac{H_c}{H_{MAC}} \dots\dots\dots (3)$$

where H_c is the measured value of heavy metals, and H_{MAC} is the maximum permissible concentration of heavy metal (MAC) of the i-th parameter. (Edet and Ofong 2002).

3.2 Geophysical Measurements

The objective of using the ERT in this study is to detect groundwater pollution resulting from the possible flow of leachate from landfills and to assesses its impact on the groundwater quality in the area. The ERT were measured along the profile between BH1 and BH2 (Figure 6) with a length of 715 m. A Lippmann 4-point light device was used for the ERT measurements. The geophysical measurements were conducted on April 29, 2021, along the right and left sides of the Takahasan stream bed.

The ERT is one of the popular methods in geophysics used for a long time (Warner, 1969; Donaldson, 1984; Adepelumi et al., 2005; Ayolabi and Daniel, 2005; Falebita et al., 2012). However, when identifying anomalies, b the characteristics of the embedded structure are not the only factors to consider; the electrode arrays used also play a crucial role. Therefore, the calculated apparent resistivity values of any ground model may vary depending on the chosen electrode arrays. For this reason, selecting an appropriate electrode array for the research is crucial for its success. The ERT measurements were carried out on a 715-m-long profile, with an electrode spacing of 5 m, using the dipole measurement technique in 6 stages. The apparent resistivity (AP) measured by the dipole-dipole electrode array were placed at the intersection point of the lines descending at an angle of 45 ° from the A, B current, and M, N voltage electrode pairs. In Figure 7, the distance between the current and voltage electrodes (AB-MN) remains constant. The ratio of the distance between the B and M electrodes (a current and an electrode) to the distance between the two current and two voltage electrodes is denoted as "n." The disadvantage of this array is that as the value of "n" increases, strong signals cannot be obtained. For instance, when the "n" value is increased from 1 to 6 while keeping the current constant, the measured potential value becomes 56 times greater (Looke 2000).

4. Results

4.1 Water Analyses

The groundwater levels and monthly precipitation (mm) are illustrated in Figure 8a (MGM, 2022). The highest groundwater level change was 33 cm in BH1 and 116 cm in BH2. Groundwater recharge area of BH1 is larger than BH2. For this reason, the groundwater level in BH1 is closer to the surface. Simple regression analyses were performed between monthly precipitation (mm) and groundwater depth in the borehole. As can be seen in Figure 8b, there is a significant relationship between groundwater level records in BH1 and monthly precipitation, with a correlation coefficient of R^2= 0.68. Figure 8c shows the simple regression analysis between groundwater level records in BH2 and monthly precipitation with a correlation coefficient R^2= 0.42. The low correlation coefficient in BH2 is due to the small size of the feeding basin and measures taken to prevent permeability in the wastage area.

Groundwater in boreholes was drained to determine hydraulic conductivity. After the drainage process was completed, the rise of the groundwater level was measured at certain time intervals. Using the Houghoudt equation (Houghoudt, 1936), hydraulic conductivity (K) was determined as 0.194 m/day, for BH1 and 0.076 m/day for BH2.

The TDS is formed by inorganic salts and small amounts of organic substances. TDS concentrations below 1000 mg/l are recommended; however, very low TDS concentrations give water a flat taste. Excessive TDS concentration increases water

MGM (2022). Turkish State Meteorological Service:https://mgm.gov.tr/eng/forecast-Citiesaspx.

hardness (WHO, 2022). The TDS results obtained in the study are given in Table 2. The highest TDS concentration was measured in the SW4S sample and does not pose any risk according to the World Health Organization (WHO) standards (2022). The Surface Water Quality Regulation (TSWQR, 2021), published in the Turkish Official Gazette dated 6/16/2021 and numbered 31513, categorizes water classes into 4 groups based on their intended use, such as high-quality (1^{st} class), less polluted (2^{nd} class), contaminated (3^{rd} class), and very polluted (4^{th} class). The tests from Ilbank (2016), the TSWQR (2021) limits, and the findings of this study are illustrated in Figure 9. As can be seen in Figure 9a, except for the SW4S sample TDS concentration, the TDS concentration of all samples was below the TDS concentration limit for 3rd class water according to TSWQR (2021).

The degree of transmission of electricity by water is called electrical conductivity. Pure water is devoid of minerals and has no conductivity. High electrical conductivity means high ion content and high TDS amount. However, the contribution of each dissolved substance to the conductivity of the water is different. Resistivity of ground, geological factors, porocity, permeability, saturation with water, distribution of water in soil, salinity and temperature increase also determine conductivity (Johansen and Carlson, 1976; Hajjar, 1997; Divya and Belagali, 2012; Demirbilek et al., 2013; Meride and Ayenew, 2016; Özel et al., 2017; Khatib et al., 2023). High electrical conductivity causes high corrosion, and low electrical conductivity increases the ability to dissolve surrounding materials. Conductivity shows the status of major ions in inorganic pollution and measures total dissolved solids and ionized species in the water. The conductivity test results of this study are all higher than the maximum limit (400 µs/cm) of WHO standards (WHO 2022). The results of analyses performed on water samples are given in Table 2.

The conductivity of the samples is shown in Figure 9b. It was observed that the conductivity of the water samples exceeded the conductivity limit set for 3rd class water in the TSWQR regulation (TSWQR 2021).

The COD measures the oxygen required to oxidize organic substances in water or wastewater (Ziyang et al., 2009). The COD values of the samples were higher than the COD limits defined in TSWQR regulation (2021). The COD values of the samples taken from the KFS outside the study area were below the COD and BOD limits defined in TSWQR regulation (Figure 9c). The BOD is the amount of oxygen bacteria need to break down organic substances under aerobic conditions and used to index the degree of organic pollution in water. While some of the organic substances are oxidized in BOD, all of them are oxidized in COD. The measured BOD value of SW2 samples in dry period was lower than the BOD value measured in the wet period (Table 2). The COD and BOD were under limit of detection in SW3 samples. The COD and BOD measured in the wet period were lower than COD and BOD measured in dry period in SW4 samples. High COD values indicate that more organic materials were hydrolyzed due to increased water input. The BOD is equal to half of COD in uncontaminated or lightly polluted waters. A low BOD/COD ratio indicates an excessive amount of non-biodegrable material (Demirbilek et al., 2013). BOD/COD ratio also shows the age of landfill. In general, aerobic, acetogenic and metanogenic phases occur in decomposition of solid wastes (Pfeffer, 1992). BOD/COD>40% in acetonic phase, BOD/COD<40% in methanogenic phase and BOD/COD<20 during methanogenic phase. In this study, the BOD/COD ratio was less than 20%, indicating that the landfill is in the methanogenic phase (Irene and Lo, 1995). Chain (1977) stated that when BOD/COD is greater than 0.5, biological treatment is more suitable. In this study, the lowest BOD/COD ratio was determined as 0.11, while the highest BOD/COD ratio was determined as 0.89. These values indicate that the acetogenic and methanogenic phases continue simultaneously due to ongoing deposition.

The pH is a logarithmic measure of the acidity or basicity of water. The variation in pH is influenced by the biological structure and diversity of wastes, as well as their dilution effects (Johansen and Carlson, 1976). As the waste site ages, the pH value tends to shift from acidic to basic.

If hydrogen ions increase, the pH of the water decreases, and the water becomes acidic. Conversely, the pH value rises when hydrogen ions increase and the water becomes alkaline. The pH of the aquatic system is an important indicator of the water quality and the extent of pollution in landfill areas and the environment. The pH concentration of water is measured on a scale ranging from 1 to 14. The pH value of pure water is equal to 7. If the pH value is less than 7, the water is acidic. If the pH value is greater than 7, the water is basic. Carbonates and bicarbonates increase the basicity of water. It should be determined whether chemicals causing high pH are harmful. Low-pH waters are corrosive and can be hazardous as they have the potential to dissolve toxic materials in their environment. The water in the region is slightly alkaline. A pH range of 6.5–8.5 is normally acceptable per WHO (2022) and TSI (2005) guidelines. The pH of all water samples was greater than 7 (Table 2). The highest pH value was 8.00, while the lowest was 7.05 (Figure 9d). Slightly alkaline character of water samples show methanogenic phase (Irene and Lo, 1995). The pH test results were within the TSWQR regulation limits.

Phenolic materials are among the chemical pollutants in wastewater. Phenol pollutants derive from the iron, steel, petrochemical, and medicine industries (Doğan, 2014). The United States Environmental Protection Agency (USEPA, 1992) and the European Union classified phenols as primary pollutants affecting human health. The number of phenolic substances in potable water should be less than 0.002 mg/lt according to TSE 266 (2005) and WHO (2022) standards. The phenolic substance amount in the water samples taken from the Eskişehir landfill drainage area was at least 0.0867 mg/l and at most 0.203 mg/l. Phenolic material concentration and ammonia nitrogen concentration in wastewater were not investigated in the study of Ilbank (2016). In Figure 9e, the phenolic material concentration limits of the TSWQR water classes are provided, along with histogram graphs illustrating the phenolic material concentrations determined in the water samples in this study. Except for the SW1 water samples, the phenolic material concentration of the other water samples contains more phenolic material than the 3rd class water quality according to TSWQR limits.

Ammonia nitrogen concentration in leachate is is a significant factor influencing environmental pollution and human health. In addition, ammonia nitrogen also affects leachate treatment processes (Haslina et al., 2021). Ammonia nitrogen is the long term stable component in the leachate (Christensen et al., 2001). As shown in Figure 9f, the ammonia nitrogen concentration of the water samples in this study was greater than the 3rd class water ammonia nitrogen concentration limits defined in TSWQR (2021).

Table 3 shows the LPI_{or}, LPI_{inor}, LPI_{hm}, and overall LPI values calculated in the SW1-May water sample and given in Figure 10. The lowest total LPI value was calculated in SW1 water sample taken from the KFS located at the upstream part of the drainage basin of the landfill. The highest LPI values were obtained from the SW2 water sample. This is likely because the BH2 borehole, from which the SW2 water sample was taken, is in close proximity to the landfill.

The LPI values of TSWQR (2021) are calculated for correlation with the LPI values of this study. As shown in Table 4, the total LPI value of the water samples was within the limits of class 4 (very polluted). The overall LPI value of the SW2 sample was 4.9 times greater than the 4^{th} class of TSWQR. The overall LPI value of the SW3 sample was 3.1 times greater than the 4^{th} class water of TSWQR, and the LPI value of the SW4 sample was 2.68 times greater than the 4^{th} class water of TSWQR.

4.2 Heavy Metal Analysis

The concentration of heavy metal elements determined in the water samples of the KFS was accepted as the concentration of heavy metal elements related to the lithological structure. As can be seen in Appendix, an increase in the concentration of Mn, Ti, Mo, B, Mg, W, Al, Fe, V, Co, Ni, Cu, Sr, Pb, Zn, Cr, Mo, Sn, and Sb metals was observed during measurement. Figure 11a shows the heavy metal concentration trendline graph for all water samples. Cu and Se concentrations were determined below the detection limit in the SW1 May sample. The Ag metal concentration was determined to be below the detection limit in the SW4 May water sample. Se, Pb, and Zn metal concentrations were determined below the limit of detection in the SW1 September sample, SW3 September sample, and SW1-SW3 September water samples, respectively. Figure 11b shows the ratio of the heavy metal concentrations of the water samples taken from KFS to those of the water samples from the study area. According to Figure 11b, the Mn, Se, Ti, Mo, Sn, Sb, B, Mg, V, Fe, Co, Ni, Cu, Sr, Pb, Bi, Zn, and Cr concentrations of the water samples taken from the study area were higher than the concentrations of the water samples taken from KFS in both the wet and dry periods. Ru, Rh, Ir, Be, Ga, Tb, Tl, Th, W, Al, Ag, and Hg concentrations increased in the wet period and decreased in the dry period. Cs and As concentrations decreased in both wet and dry periods.

The correlation with water quality is given in Table 5. The metal concentrations determined from the water samples belonging to the study area are in good agreement with the limits established by the TSWQR (2021).

According to the metal limits defined by WHO (2022) for potable and usable water given in Table 6, The highest Ni concentration determined in this study was higher than the Ni concentration limit defined by WHO (2022).

Here, the HPI and HEI were calculated using the ratios of measured heavy metal concentrations to the limits established by the TSWQR (2021). Figure 12a indicates that the calculated HPI values were under 100 in this study. The HEI gives the general evaluation of heavy metal risk in water concentration. Fig. 10b shows that the SW1, SW3 and SW4 samples were in “very pure-pure” zone, where as SW2 sample is in “slightly effected” zone.

As can be seen in Figure 12a, all samples were under the upper level of low risk zone for both periods. The TSWQR values (for S_i values 4th class, for I_i values 1st class) were based on the calculations. The SW2 shows the highest degree in dry period. The others yielded similar results. The HEI values were similar to HMPI, however SW2 exhibits slightly affected (Class III, Caeiro et al., 2005). SW1, SW3 and SW4 show very pure in wet period (Class I). These samples fall into the pure zone in dry period (Class II). These results show a consistency in terms of TSWQR.

Figure 13 shows the relationship between total metal content and pH. All the samples locates near "near neutral, high metal location except SW3 sample, which locates between near neutral-high metal and acid-high metal location. High metal content in water samples can pose serious health risks for consumers (Ficklin et al. 1992; Caboi et al. 1999).

4.3 Geophysical Measurements

Dissolved waste material is directly related to electrical conductivity and resistivity. Given that leachate contains a high concentration of ions, water pollution may be to blame for the low electrical resistivity and high conductivity (Meju, 2000; Bernstone et al., 2000; Kjeldsen et al., 2002; Rosqvist et al., 2003). However, geophysical methods alone are not always sufficient in this regard. Geophysical methods can be used together with chemical and hydrogeological methods to investigate groundwater pollution. There are many geophysical studies on this subject (Meju, 2000; Karlık and Kaya, 2001; Baba et al., 2004; Kaya et al., 2007; Boudreault et al., 2010; Vaudelet et al., 2011; Haile and Abiye, 2012; De Carlo et al., 2013; Ayolabi et al., 2013; Kaya et al., 2014; Tsourlos et al., 2014; Wijesekara et al., 2014; Konstantaki et al., 2015; Chira Oliva et al., 2015; Gómez-Puentes et al., 2016; Ganiyu et al., 2016; Çınar et al., 2016; Soupios and Ntarlagiannis, 2017; Kayode et al., 2018; Di Maio et al., 2018; Akintorinwa and Okoro, 2019).

Right and left side ERT measurement profiles were given Figure 14. It was observed that the resistivity records taken on the right side ERT measurements are slightly different especially at near-surface levels. The ERT measurements emphasize a slight difference between the left and right side records regarding contamination. The measurements can be grouped as low resistivity values (<5 ohms.m.) significantly observed in the region close to the landfill area, moderate resistivity values (10–20 ohms.m.), and relatively high resistivity values as a thin layer close to the surface (>20 ohms.m.). Soils with low resistivity are notably laterally wider, particularly in the regions close to the landfill area, up to 130 meters. Intensive contamination is remarkable between 40 and 80 meters horizontally. The contamination, thought to be caused by leachate water accumulation. High contaminated zones like a plume which disconnected with each other. Shape and volumes of high contaminated zones gets smaller towards the BH1. The presence of sandy, silty litology observed at surface in the region causes the leachate water to flow the deep levels due to their high permeability. Low resistivity values are rarely observed in the continuation of the measurement zone away from the landfill area. Conversely, areas with high resistivity are monitored at a narrow depth, almost the entire measurement line at near-surface levels. The recording of high resistivity values near the surface may be related to surface water flow throught landwill to the BH1 (Ganiyu et al., 2016). Left-side records show the high contamination observed at the deeper levels near the landfill area. The levels are considered to be saturated with leachate water, distinguished by low resistivity values, are still remarkable but spread up to 95 meters horizontally from the landfill area.

A total of four profiles with various depths of the Takahasan Stream bed were obtained in Surfer 8 to analyze the contamination change. Near-surface heterogeneity is also evident at 1.2 meters of depth, as shown in Figure 15. The increase in contaminated areas with low resistivity is highlighted more prominently. It was determined that locations near the landfill area were significantly affected by leachate water. A remarkable decrease was observed in the resistivity values from 12.76 meters and continues slightly down to the 31.80 meters depth (Figure 15b–d).

5. Conclusion

This study investigated possible surface water and groundwater pollution in the Eskişehir city landfill drainage area. This area was used as a wild storage area before 2016. After 2016, it was transferred to a regular waste storage area. Two boreholes at 30 m depth were drilled in the Eskişehir landfill drainage basin. Groundwater and surface water samples were collected in 2021, both during wet and dry periods. In addition, water samples were taken from the water source of the Kadirbey farm area, which is at the upstream part of the landfill area drainage basin.

The TDS concentration of all water samples except one was lower than the 3rd class water TDS concentration limits defined by TSWQR (2021). The conductivity limits are within the boundaries of 3rd class water quality according to the limits set by the TSWQR (2021).

In addition, the conductivity values of water samples were higher than the conductivity limits of the WHO (2022). The COD values of the water samples taken in the landfill basin area are higher than the COD limits of the TSWQR (2021) regulation. A high ratio of COD to BOD values indicates the presence of excessive organic pollution in water samples. The highest pH of the water samples taken from the study area was 8.73, while the lowest was 8.00. According to TSWQR regulation on pH limits, the pH test results of water samples were alkaline in nature. The quality of spring water in the Kadirbey area is determined to be a 1^{st} class water source, according to TSWQR (2021). The analysis results on the samples taken from the KFS represent that the region is not affected by the landfill pollution.

Mn, Se, Ti, Mo, Sn, Sb, B, Mg, V, Fe, Co, Ni, Cu, Sr, Pb, Bi, Zn, and Cr concentrations in the water samples taken from the study area were increased during testing periods. However, according to the TSWQR (2021) and heavy metal concentration limits defined by the WHO (2022), the heavy metal concentration values determined in the water samples were within limits, except for nickel concentration.

Inorganic material leachate pollution index (LPI_{inor}), organic material leachate pollution index (LPI_{or}), heavy metal pollution index (LPI_{hm}), and overall Leachate Pollution Index are calculated (LPI). The overall LPI value of the SW2 sample is 4.9 times greater than the 4^{th} class water of TSWQR. The overall LPI value of the SW3 sample is 3.1 times greater than the 4^{th} class water of TSWQR, and the LPI value of the SW4 sample is 2.68 times greater than the 4^{th} class water of TSWQR.

According to the HPI and HEI indexes, which provide an overall evaluation, the results of the heavy metal analyses do not appear to pose significant risks.

The ERT records show a decrease in resistivity with depth. This may result from the pollution formed during wild storage along the Takahasan Stream and lithological structure. The presence of water pollution accumulation is indicated by the low resistivity observed from the surface to depth near the waste storage area. However, a decrease in water pollution is observed both at the surface and at depth as one moves horizontally. Slight differences may arise in the lateral distribution of permeability. But the more acceptable explanation for the small and disconnected high contaminated water areas in ERT records is that these contaminated areas may be the remnants of former wild waste landfill area. Because of the unrestrained waste storage in the past, the high level contamination was occurred and today we can see in the ERT measurement as small patches of contaminated areas away from the landfill.

While chemical and hydrogeological analyses only provide information on water content and movement of water underground, geophysical measurements can be affected by the rock or ground properties that make up the environment, as well as groundwater. Lower groundwater level, lower hydraulic conductivity, higher clay content in weathered part in BH2 with respect to BH1 caused to change the electrical conductivity. In the past, anthropogenic processes, such as burning tires and electric cables, were carried out in the area close to BH2, which may have caused a decrease in electrical conductivity. Additionally, the differences in electrical resistivity may be attributed to the fact that BH1 is farther from the landfill site and is fed by groundwater from side drainage flows that are not contaminated by landfill leachate. As a result, geophysical measurements alone may be insufficient in environmental pollution research. Therefore, studies should be supported by other methods.

It is suggested that the concentration of pollution parameters in the study area should be monitored according to related soil and water pollution regulations at least at one-year intervals. These observations may help with surface water and groundwater conservation efforts.

Acknowledgements

The authors would like to express their sincere thanks to Eskisehir Osmangazi University Scientific Research Projects Coordination Unit for support this study.

Author Contributions

All authors contributed to the conception and design of the study. Conceptualization, methodological study and sample preparation were done by AK, field work was done by AK and OTS, evaluation of the experimental results was done by AK, OTS and CG. The first draft was written by AK, OTS and CG. All authors read and approved the final manuscript.

Funding

This work has been supported by Eskisehir Osmangazi University Scientific Research Projects Coordination Unit under grant number (Project ID:121, No: 2020-15056)

Data Availability All data generated or analysed during this study are included in this published article.

Declarations

Competing interests On the behalf of all authors, the corresponding author states that there are no competing interests related to this work.

References

Adepelumi AA, Ako BD, Afolabi O, Arubayi JB (2005). Delineation of contamination plume around oxidation sewage-ponds in Southwestern Nigeria. Environmental Geology 48 (8): 1137–1146. https://doi.org/ 10.1007/s00254-005-0056-5

Akintorinwa OJ, Okoro OV (2019). Combine electrical resistivity method and multi-criteria GIS-based modeling for landfll site selection in the Southwestern Nigeria. Environmental Earth Sciences 78: 162. https://doi.org/10.1007/s12665-019-8153-z

Ayolabi EA, Daniel YP (2005). Hydro-chemical and electrical resistivity assessment of the impact of the solid waste on the groundwater at OkeAlfa refuse dump-site, Lagos, Nigeria. Environmental Science and Engineering Technology 12: 5936–5946

Ayolabi EA, Folorunso AF, Kayode OT (2013). Integrated geophysical and geochemical methods for environmental assessment of Municipal Dumpsite System. International Journal of Geosciences 4: 850–862. https://doi.org/10.4236/ijg.2013.45079

Baba A, Kavdir Y, Deniz O (2004). The impact of an open waste disposal site on soil and groundwater pollution. International Journal of Environment and Pollution 22 (6): 676-687. https://doi.org/10.1504/IJEP.2004.006057

Baccini P, Henseler G, Figi R, Belevi H (1987). Water and element balances of municipal solid waste landfills. Waste Management & Research 5: 483–499. https://doi.org/10.1177/0734242X8700500162

Bernstone C, Dahlin T, Ohlsson T, Hogland W (2000). DC-resistivity mapping of internal landfill structures: two pre-excavation surveys. Environmental Geology 39 (3–4): 360–371. https://doi.org/10.1007/s002540050015

Boudreault JP, Dubé JS, Chouteau M, Winiarski T, Hardy É (2010). Geophysical characterization of contaminated urban fills. Engineering Geology 116: 196–206. https://doi.org/10.1016/j.enggeo.2010.09.002.

Caboi R, Cidu R, Fanfani L, Lattanzi P, Zuddas P (1999). Environmental mineralogy and geochemistry of the abandoned Pb–Zn Montevecchio-Ingurtosu mining district, Sardinia, Italy. Chronique de la rechérche miniére 534: 21–28

Caeiro S, Costa MH, Ramos TB, Fernandes F, Silveria N et al. (2005). Assessing heavy metal contamination in Sado Estuary sediment: an index analysis approach. Ecological Indicators 5 (2):151-169. https://doi.org/10.1016/j.ecolind.2005.02.001

Chain ESK (1977). Stability of organic matter in leachates. Water Research 11:225, 32. https://doi.org/10.1016/0043-1354(77)90130-0

Chira Oliva P, Barbalho DP, Cruz JR (2015). Environmental study of the Bragança City landfill (Brazil) applying Ground Penetrating Radar. EAGE, 21st European Meeting of Environmental and Engineering Geophysics doi:https://doi.org/10.3997/2214-4609.201413820

Christensen TH, Kjeldsen P, Bjerg PL, Jensen DL, Christensen JB et al. (2001). Biogeochemistry of landfill leachate plumes. Applied Geochemistry 16: 659–718. https://doi.org/10.1016/S0883-2927(00)00082-2

Çelik M, Tastekin M, Kayabalı K (2007). An investigation of the surface and groundwater leachate from an old waste disposal site at Mamak, Ankara, Turkey. International Journal of Environment and Pollution 30 (3-4): 548-560. https://doi.org/10.1504/IJEP.2007.014828

Çetin M, Jawed AA (2021). The chancing of Mg concentrations in some plants grown in Pakistan depends on plant spcies and the growing environment. Kastamonu University Journal of Engineering and Sciences 7 (2): 167–174.

Çetin M (2020). The changing of important factors in the landscape planning occur due to global climate change in temperature, rain and climate types: A case study of Mersin

City. Turkish Journal of Agriculture-Food Science and Technology 8 (12): 2695–2701. https://doi.org/10.24925/turjaf.v8i12.2695-2701.3891

Çetin M, Zeren I, Sevik H, Cakir C, Akpinar H (2018). A study on the determination of the natural park's sustainable tourism potential. Environmental Monitoring Assessment 190 (3): 1–8. https://doi.org/10.1007/s10661-018-6534-5

Çınar H, Altundas S, Ersoy E, Bak K, Bayrak N (2016). Application of two geophysical methods to characterize a former waste disposal site of the Trabzon- Moloz district in Turkey. Environmental Earth Sciences 75 (52). https://doi.org/10.1007/s12665-015-4839-z

Daniel DE (1993). Geotechnical practice for waste disposal. In: Daniel DE (ed) Geotechnical practice for waste disposal. Springer, US. https://doi.org/10.1007/978-1-4615-3070-1

De Carlo L, Perri MT, Caputo MC, Deiana R, Vurro M et al. (2013). Characterization of a dismissed landfll via electrical resistivity tomography and mise-à-la-masse method. Journal of Applied Geophysics 98: 1–10. https://doi.org/10.1016/j.jappgeo.2013.07.010

Demirbilek D, Öztüfekçi Önal A, Demir V, Uslu G, Arslanoglu-Isık H (2013). Characterization and pollution potential assessment of Tunceli, Turkey municipal solid waste open dumping site leachates. Environmental Monitoring and Assessment 185: 9435-9449. https://doi.org/10.1007/s10661-013-3263-7

Di Maio R, Fais S, Ligas P, Piegari E, Raga R et al. (2018). 3D geophysical imaging for site-specific characterization plan of an old landfill. Waste Management 76: 629–642. https://doi. org/10.1016/j.wasman.2018.03.004.

Divya J, Belagali SL (2012). Impact of chemical fertilizers on water quality in selected agricultural Areas of Mysore District, Karnataka, India. Agris On-line Papers in Economics and Informatics 2 (3): 1449–1458. https://doi.org/10.6088/ijes.002020300030

Doğan T (2014). Atık Sulardan Fenolik Bileşiklerin Uzaklaştırılması için Yeni Nesil Destek Malzemeleri. Master of Science, Department of Chemistry, openaccess.hacettepe.edu.tr (In Turkish).

Donaldson JS (1984). Electrical methods of detecting contaminated groundwater at the Stringfellow waste disposal site, Riverside County, California. Environmental Geology 6: 11-20

Edet AE, Offiong OE (2002). Evaluation of water quality pollution indices for heavy metal contamination monitoring: A study case from Akpabuyo-Odukpani area, lower Cross River basin (southeastern Nigeria). Geological Journal 57: 295–304. https://doi.org/10.1023/B:GEJO.0000007250.92458.de

Falebita DE, Bayowa OG, Olorunfemi MO, Adepelumi AA (2012). Groundwater contamination prediction using finite element derived geoelectric parameters constrained by chemical analysis around a sewage site, Southwestern Nigeria. International Journal of Geosciences 3: 404–409. https://doi.org/10.4236/ijg.2012.32045

Ficklin DJWH, Plumee GS, Smith KS, McHughb JB (1992). Geochemical classification of mine drainages and natural drainages in mineralized areas. In: Kharaka YK, Maest AS (eds) Water–rock interaction, vol 7. Balkema, Rotterdam, pp 381–384

Ganiyu SA, Badmus BS, Oladunjoye MA, Aizebeokhai AP, Ozebo VC et al. (2016). Assessment of groundwater contamination around active dumpsite in Ibadan southwestern Nigeria using integrated electrical resistivity and hydrochemical methods. Environmental Earth Sciences 75 (8). https://doi.org/10.1007/ s12665-016-5463-2

Gómez-Puentes FJ, Pérez-Flores MA, Reyes-López JA, Lopez DL, Herrera-Barrientos F et al. (2016). Geochemical modeling and low-frequency geoelectrical methods to evaluate the impact of an open dump in arid and deltaic environments. Environmental Earth Sciences 75: 1062. https://doi.org/10.1007/s1266 5-016-5860-6

Gözler MZ, Cevher F, Küçükayman A (1985). Eskişehir civarının jeolojisi ve su kaynakları. MTA Dergisi 103/104: s. 40–54, Ankara.

Haile T, Abiye TA (2012). Environmental impact and vulnerability of the surface and ground water system from municipal solid waste disposal site: Koshe, Addis Ababa. Environmental Earth Sciences 67: 71–80. https://doi.org/10.1007/s12665-011-1480-3.

Hajjar ZK (1997). Lebanese water and peace in the Middle East. Dar el ilm lilmalayin

Han Z, Ma H, Shi G, He L, Wei L et al. (2016). A review of groundwater contamination near municipal solid waste landfill sites in China. Science of the Total Environment 569–570: 1255–1264, https://doi.org/10.1016/J.SCITOTENV.2016.06.201

Horton RK (1965). An index-number system for rating water quality. Journal of the Water Pollution Control Federation 37: 300–306.

Houghoudt SB (1936). Bijdragen tot de kennis van eenige natuur kundige grootheden van den grond, 4 Versl. Lamdb., Ond. 42 (13) B: 449—451, Algemeene Landsdrukkerji, The Hague.

İlbank (2016). Rehabilitation Of Eskişehir Municipality Old Waste Site Feasibility and Final Project and Final Project Former leachate water of wastage treatmant plant Final Project preparation Report (Soil Survey and Evaluation Report). Contractor Piramit AŞ. B Zorlu (Geology Engineer), S Çetin (Environment Engineer) and A Bilgin (Civil Engineer).

Johansen OJ, Carlson DA (1976). Characterization of sanitary landfill leachates. Water Research 10: 1129–1134. https://doi.org/10.1016/0043-1354(76)90046-4

Kamaruddin MA, Yusof MS, Rui LM, Isa AM, Zawawi MH et al. (2017). An overview of municipal solid waste management and landfill leachate treatment: Malaysia and Asian perspectives. Environmental Science and Pollution Research 24 (35):26988–27020. https://doi.org/10. 1007/s11356-017-0303-9

Kara H, Demir Yetis A, Temel H (2021). Assessment of heavy metal contamination in groundwater of Diyarbakir Oil Production Area, (Turkey) using pollution indices and chemometric analysis. Environmental Earth Sciences 80: 1-15. https://doi.org/10.1007/s12665-021-10011-2

Kaya MA, Özürlan G, Şengül E (2007). Delineation of soil and groundwater contamination using geophysical methods at a waste disposal site in Çanakkale, Turkey. Environmental Monitoring and Assessment 135: 441–444. https://doi.org/10.1007/s10661-007-9662-x

Kaya MA, Özürlan G, Balkaya Ç (2014). Geoelectrical investigation of seawater intrusion in the coastal urban area of Çanakkale, NW Turkey. Environmental Earth Sciences 73: 1151-1160. https://doi.org/10.1007/s1266 5-014-3467-3

Karlık G, Kaya MA (2001). Investigation of groundwater contamination using electric and electromagnetic methods at an open waste-disposal site: a case study from Isparta, Turkey. Environmental Geology 40: 725–731. https://doi.org/10.1007/s002540000232

Kayode OT, Okagbue HI, Achuka J (2018). Water quality assessment for groundwater around a municipal waste dump site. Data in Brief 17: 579–587. https://doi.org/10.1016/j.dib.2018.01.072

Khatib M, Daoud M, Arairo W, Saba M, Mortada H (2023). Evaluation of Water Quality in the South of Lebanon: Case Study. Water, Air, & Soil Pollution 234 (7): 410. https://doi.org/10.1007/s11270-023-06453-y

Kjeldsen P, Barlaz MA, Rooker AP, Baun A, Ledin A et al. (2002). Present and Long-Term Composition of MSW landfill leachate: a review. Critical Reviews in Environmental Science and Technology 32 (4): 297-336. https://doi.org/10.1080/10643380290813462

Koç I (2021). Using Cedrus atlantica's annual rings as a biomonitor in observing the changes of Ni and Co concentrations in the atmosphere. Environmental Science and Pollution Research 1–7. https://doi.org/10.1007/s11356-021-13272-3

Konstantaki LA, Ghose R, Draganov D, Diaferia G, Heimovaara T (2015). Characterization of a heterogeneous landfll using seismic and electrical resistivity data. Geophysics 80 (1):13–25. https://doi.org/10.1190/geo2014-0263.1

Kumar D, Alappat BJ (2005a). Evaluating leachate contamination potential of landfill sites using leachate pollution index. Clean Technologies and Environmental Policy 7: 190–197. https://doi.org/10.1007/s10098-004-0269-4

Kumar D, Alappat BJ (2005b). Analysis of leachate pollution index and formulation of sub leachate pollution indices. Waste Management & Research 22: 230–239. https://doi.org/10.1177/0734242X05054875

Kumar D, Alappat BJ (2005c). Errors involved in the estimation of leachate pollution index. Journal of Hazardous, Toxic, and Radioactive Waste 9: 103–111. https://doi.org/10.1061/(ASCE)1090-025X(2005)9:2(103

Meju MA (2000). Geoelectrical investigation of old/abandoned, covered landfill sites in urban areas: model development with a genetic diagnosis approach. Journal of Applied Geophysics 44: 115-150. https://doi.org/10.1016/S0926-9851(00)00011-2

Meride Y, Ayenew B (2016). Drinking water quality assessment and its effects on residents health in Wondo genet campus, Ethiopia. Environmental Systems Research 5 (1): 1-7. https://doi.org/10.1186/s40068-016-0053-6

Mohan SV, Nithila P, Reddy SJ (1996). Estimation of heavy metals in drinking water and development of heavy metal pollution index. Journal of Environmental Science and Health Part A: Toxic/hazardous substances and environmental engineering 31 (2):283–289. https://doi.org/10.1080/10934529609376357

Muttamara S, Leong ST (1997). Environmental monitoring and impact assessment of a solid waste disposal site. Environmental Monitoring and Assessment 48: 1–24. https://doi.org/10.1023/A:1005744601984

Niininen M, Kalliokoski P (1993). Quality of landfill leachates and their effect on groundwater, Green 1993. International Symposium on Geotechniques Related to the Environment, Waste Disposal by Landfill v.2: 28 June, Bolton Institute.

Pfeffer JT (1992). Solid waste management engineering. Englewood Clifs, NJ: Prentice Hall.

Rizwan R, Gurdeep S, Manish Kumar J (2011). Application of heavy metal pollution index for ground water quality assessment in Angul district of Orissa, India. International Journal of Research in Chemistry and Environment 1 (2): 118–122

Rosqvist H, Dahlin T, Fourie A, Röhrs L, Bergtsson A et al. (2003). Proceedings Sardinia, Ninth International Waste Management and Landfill Symposium. CISA Publisher, Italy, pp. 27-36

Sevik H, Cetin M, Ucun Ozel H, Ozel HB, Mossi MMM et al. (2020a). Determination of Pb and Mg accumulation in some of the landscape plants in shrub forms. Environmental Science and Pollution Research 27 (2): 2423–2431. https://doi.org/10.1007/s11356-019-06895-0

Sevik H, Cetin M, Ozel HB Akarsu H, Zeren Cetin I 2020b. Analyzing of usability of tree-rings as biomonitors for monitoring heavy metal accumulation in the atmosphere in urban area: a case study of cedar tree (Cedrus sp.). Environmental Monitoring and Assessment 192 (1): 1–11. https://doi.org/10.1007/s10661-019-8010-2

Sharma A, Ganguly R, Gupta AK (2019). Characterization and energy generation potential of municipal solid waste from nonengineered landfll sites in Himachal Pradesh, India. Journal of Hazardous, Toxic, and Radioactive Waste 23 (4): 04019008. https://doi.org/10.1061/(ASCE) HZ.2153-5515.0000442.

Sirajudeen J, Arul Manikandan S, Manivel V (2014.) Heavy metal pollution index of ground water of Fathima Nagar area near Uyyakondan Channel, Tiruchirapalli District, Tamilnadu, India. World Journal Pharmacy and Pharmaceutical Science 4 (1): 967–975.

Soupios P, Ntarlagiannis D (2017). Characterization and monitoring of solid waste disposal sites using geophysical methods: current applications and novel trends. In: Sengupta D, Agrahari S (eds) Modelling Trends in Solid and Hazardous. Waste Management Springer, Singapore, pp 75–103. https://doi.org/10.1007/978-981-10-2410-8_5

Tamasi G, Cini R (2003). Heavy metals in drinking waters from Mount Amiata (Tuscany, Italy). Possible risks from arsenic for public health in the Province of Siena. Science of The Total Environment 327: 41–51. https://doi.org/10.1016/j.scitotenv.2003.10.011

Tamru AT, Chakma S (2015). Mathematical modelling for landfill leachate pollution index error estimation. Discovery 41 (189): 123-129.

TS 2789+T1 (2011). Water quality-Determination of Chemical Oxygen Demand. Turkish Standard.

TSE 266 (2005). Türk Standartları Enstitüsü, Sular-İnsani tüketim amaçlı sular. Türk Standartları Enstitüsü, ICS 13.060.20 (In Turkish).

TS EN ISO 10523 (2012). Water quality. Determination of pH is classified in these ICS categories:13.060.50 Examination of water for chemical substances.

TS ISO 5667-10 (2021). Water quality-Sampling-Chapter 10: Guidance on sampling wastewater.

Tsourlos P, Vargemezis GN, Fikos I, Tsokas GN (2014) DC geoelectrical methods applied to landfll investigation: case studies from Greece. First Break 32 (8): 81–89. https://doi.org/10.3997/1365-2397.32.8.76968

TSWQR (2021). Turkey's Surface Water Quality Regulation, published in the Official Gazette dated 16/6/2021 and numbered 31513 (in Turkish).

Ucun Ozel H, Ozel HB, Cetin M, Sevik H, Gemici BT et al. (2019). Base alteration of some heavy metal concentrations on local and seasonal in Bartin River. Environmental Monitoring and Assessment 191 (9): 594. https://doi.org/10.1007/s10661-019-7753-0

USEPA (1992). United States Environmental Protection Agency, Decision Makers Guide to Solid Waste Managements.

Varol T, Cetin M, Ozel HB, Sevik H, Zeren Cetin I (2022). The effects of climate change scenarios on Carpinus betulus and Carpinus orientalis in Europe. Water, Air, Soil Pollution 233 (2): 1–13. https://doi.org/10.1007/s11270-022-05516-w

Vaudelet P, Schmutz M, Pessel M, Franceschi M, Guérin R et al. (2011). Mapping of contaminant plumes with geoelectrical methods. A case study in urban context. Journal of Applied Geophysics 75: 738–751. https:// doi.org/10.1016/j.jappgeo.2011.09.023.

Ziyang L, Youcai Z, Tao Y, Yu S, Huili C et al., (2009). Natural attenuation and characterization of contaminants composition in landfill leachate under different disposing ages. Science of the Total Environment, 407: 3385–3391. https://doi.org/10.1016/j.scitotenv.2009.01.028

Warner DL (1969) Preliminary field studies using earth resistivity measurements for delineating zones of contaminated ground water. Groundwater 7 (1): 9–16. https://doi.org/10.1111/j.1745-6584.1969.tb01262.x

WHO (2022). Guidelines for drinking water quality, fourth edition incorporating the first and second addenda, Geneva: World Health Organization; Licence: CC BY-NC-SA 3.0 IGO, Switzerland.

Wijesekara SSRMDHR, Mayakaduwa SS, Siriwardana AR, de Silva N, Basnayake BFA et al. (2014). Fate and transport of pollutants through a municipal solid waste landfll leachate in Sri Lanka. Environmental Earth Sciences 72: 1707-1719. https://doi.org/10.1007/ s12665-014-3075-2

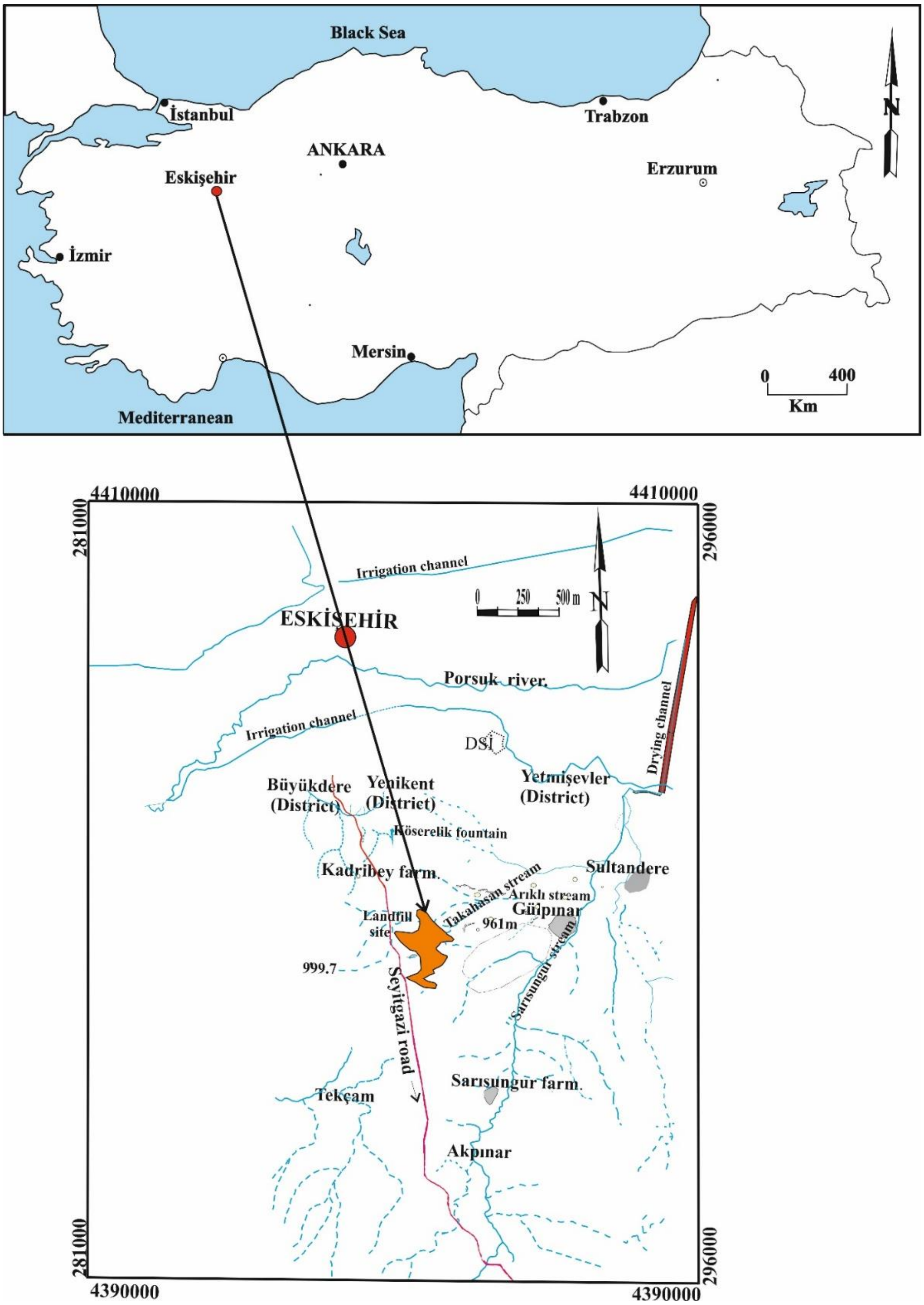

Figure 1. Location map of Eskişehir landfill site

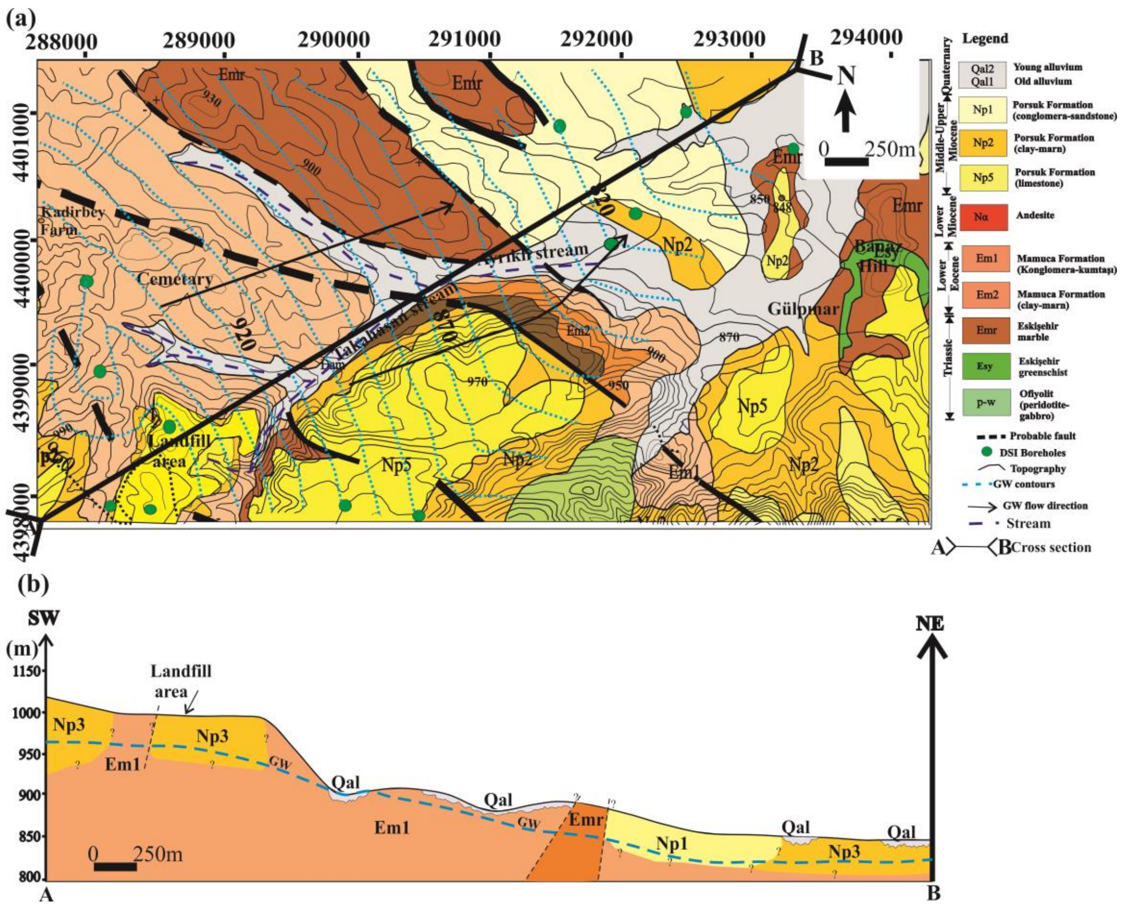

Figure 2. a) The study area geology, topography and groundwater flow map vicinity (geology map modified from Gözler et al., 1985); b) SW-NE oriented geological section of the area.

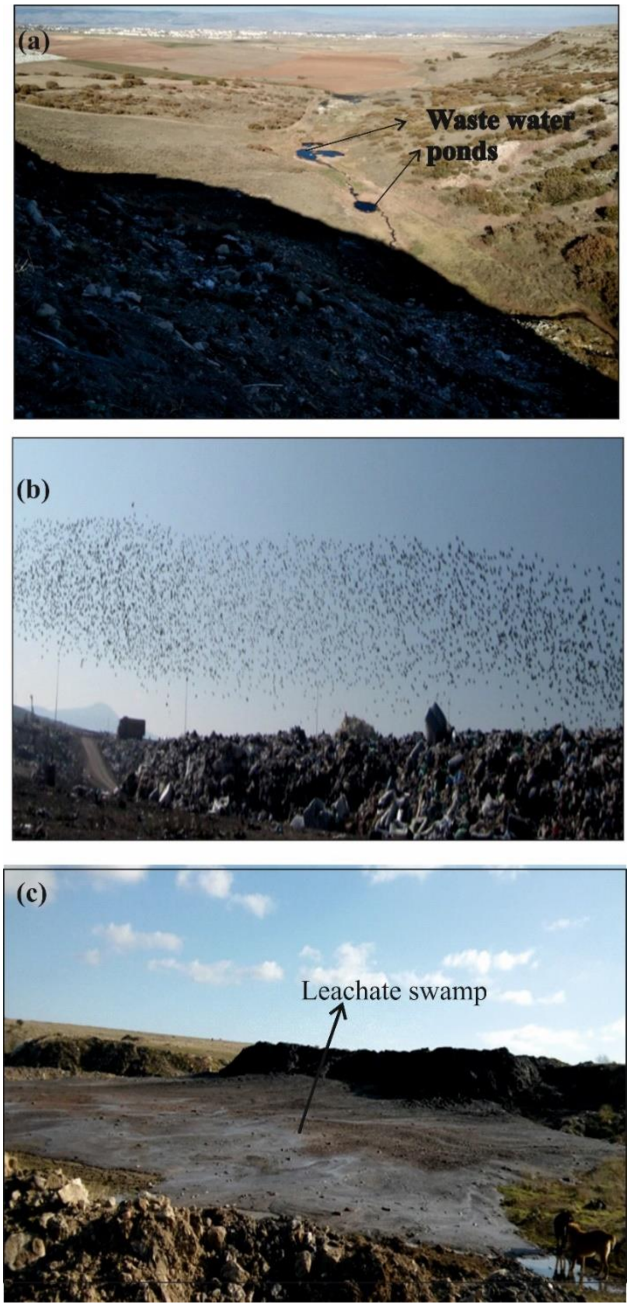

Figure 3. Views from previous irregular landfill a) waste water ponds along the Takahasan stream bed, b) garbage disposal and wildlife, c) leachate swamp.

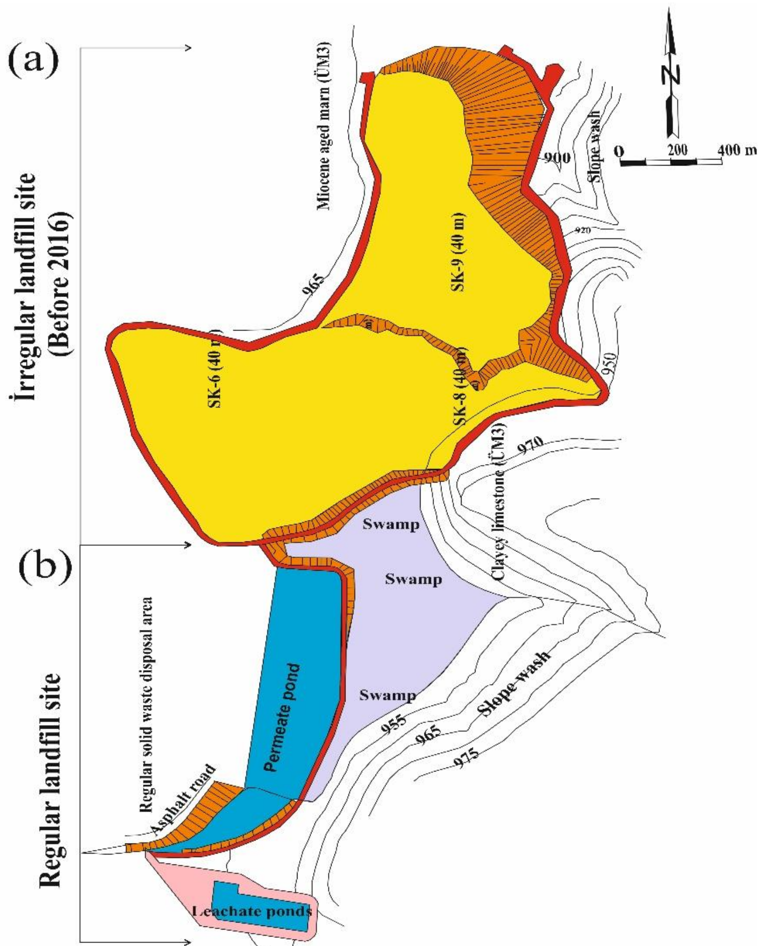

Figure 4. Plan map of regular and irregular landfill site (İlbank, 2016) a) rehabilitated irregular landfill area b) regular landfill area

Figure 5. a) A view of Eskişehir regular landfill from west to east direction, b) a view of Eskişehir regular landfill from south to north direction, c) a view of Eskişehir landfill from north to south direction.

Table 1 Water sample locations and sampling dates

Location	Coordinates	Water samples	Sampling date
Kadirbey farm	288289.49E	SW1M	May 2021
	4399119,59N	SW1S	September 2021
BH1	290027,29E	SW3M	May 2021
	4398950,41N	SW3S	September 2021
BH2	290357,54E	SW2M	May 2021
	4399321,73N	SW2S	September 2021
Surface water	290027,29E	SW4M	May 2021
	4398950,41N	SW4S	September 2021

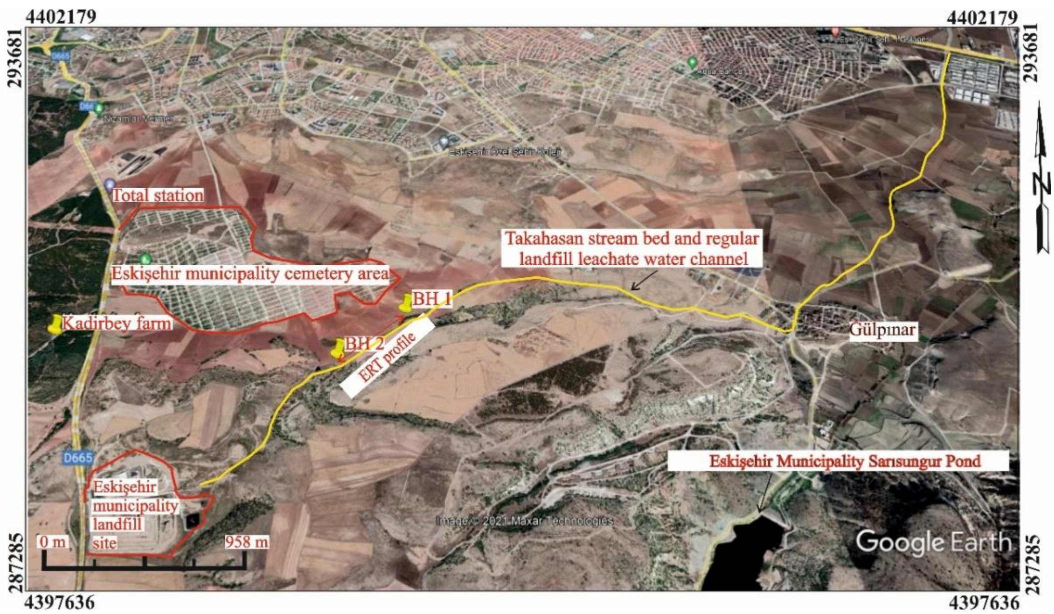

Figure 6. ERT profile on Google Earth image.

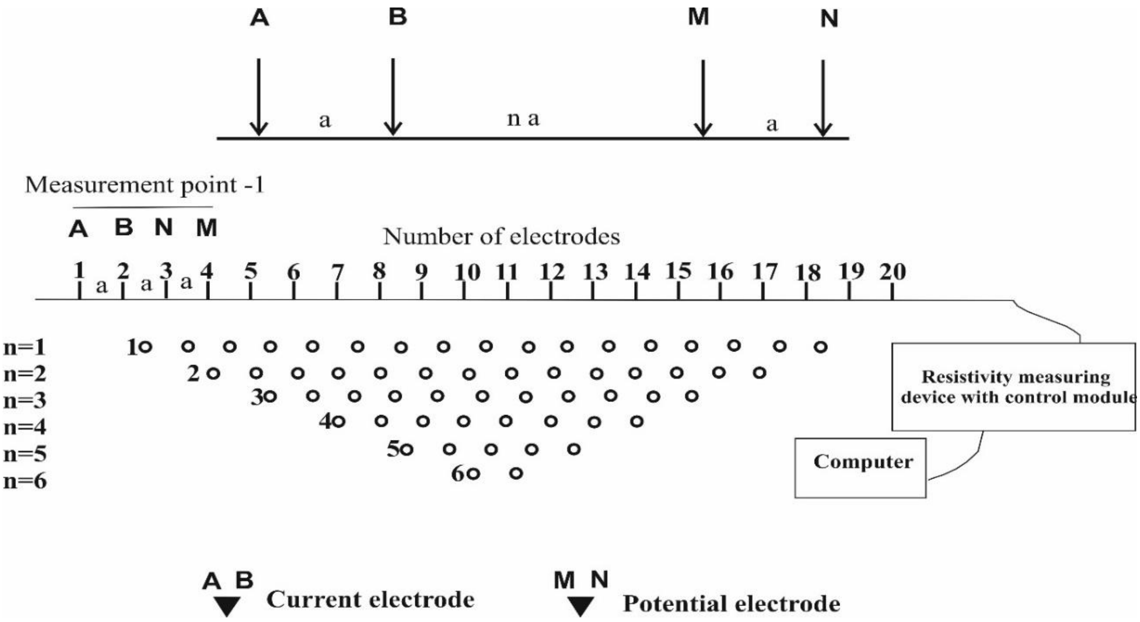

Figure 7. Schematic representation of dipole - dipole array (after Looke, 2000).

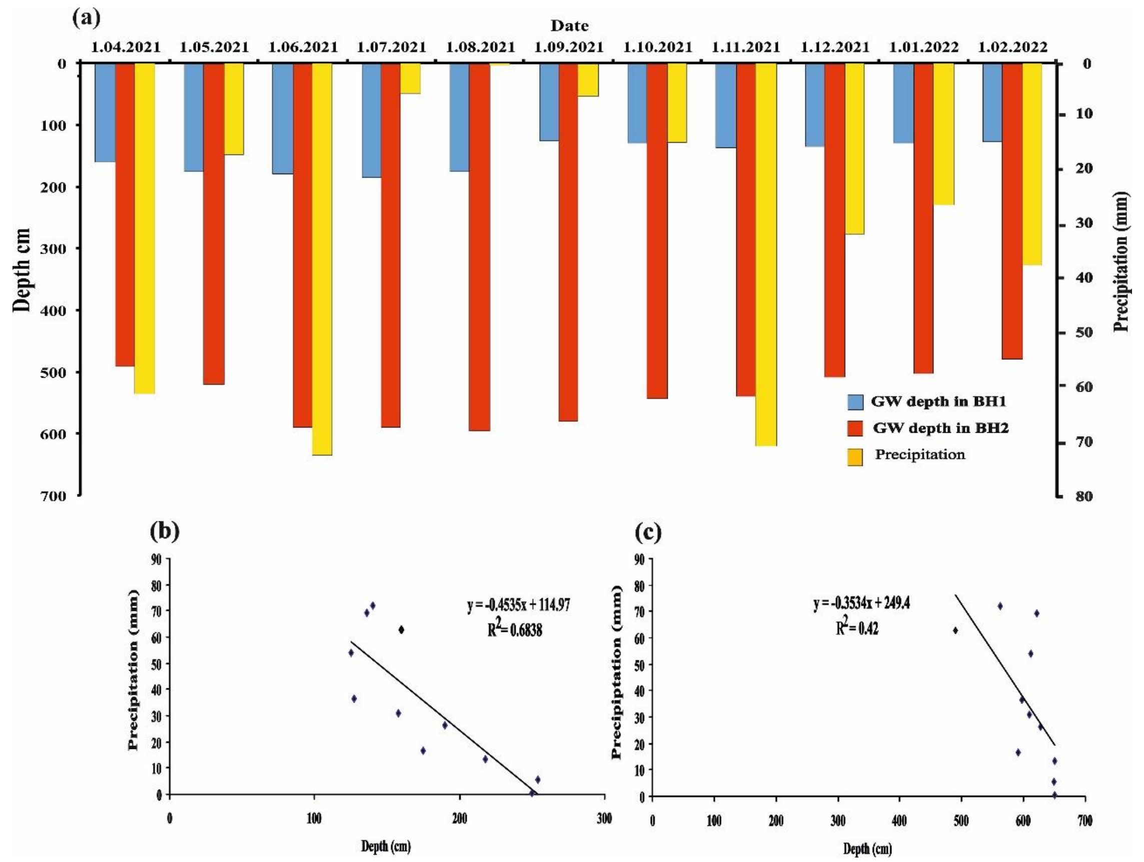

Figure 8. Graph showing a) groundwater level records in boreholes and monthly precipitation, b) simple regression analysis between montly precipitation and groundwater depth records from BH1, c) simple regression analysis between montly precipitation and groundwater level records from BH2.

Table 2 Water samples test results

Sample	TDS	pH	Phenol	Conductivity	COD	BOD	Ammonia	BOD/COD
SW1M	100	7.99	0.0018	449	<LOQ*	<LOQ**	12	-
SW1S	175	8.05	0.0019	435	<LOQ*	<LOQ**	8	
SW2M	750	7.05	0.0938	853	92.744	56.53	968	0.61
SW3M	678	7.90	0.192	958	91.759	<LOQ**	1387	-
SW3S	750	7.82	0.136	960	<LOQ*	<LOQ**	398	-
SW4M	989	7.85	0.203	1228	88.500	67.87	258	0.77
SW4S	1189	8.00	0.168	1356	97.500	86.92	367	0.89

(LOQ:Limit of Detection ,*LOQ= 20.55, **LOQ=4.85)

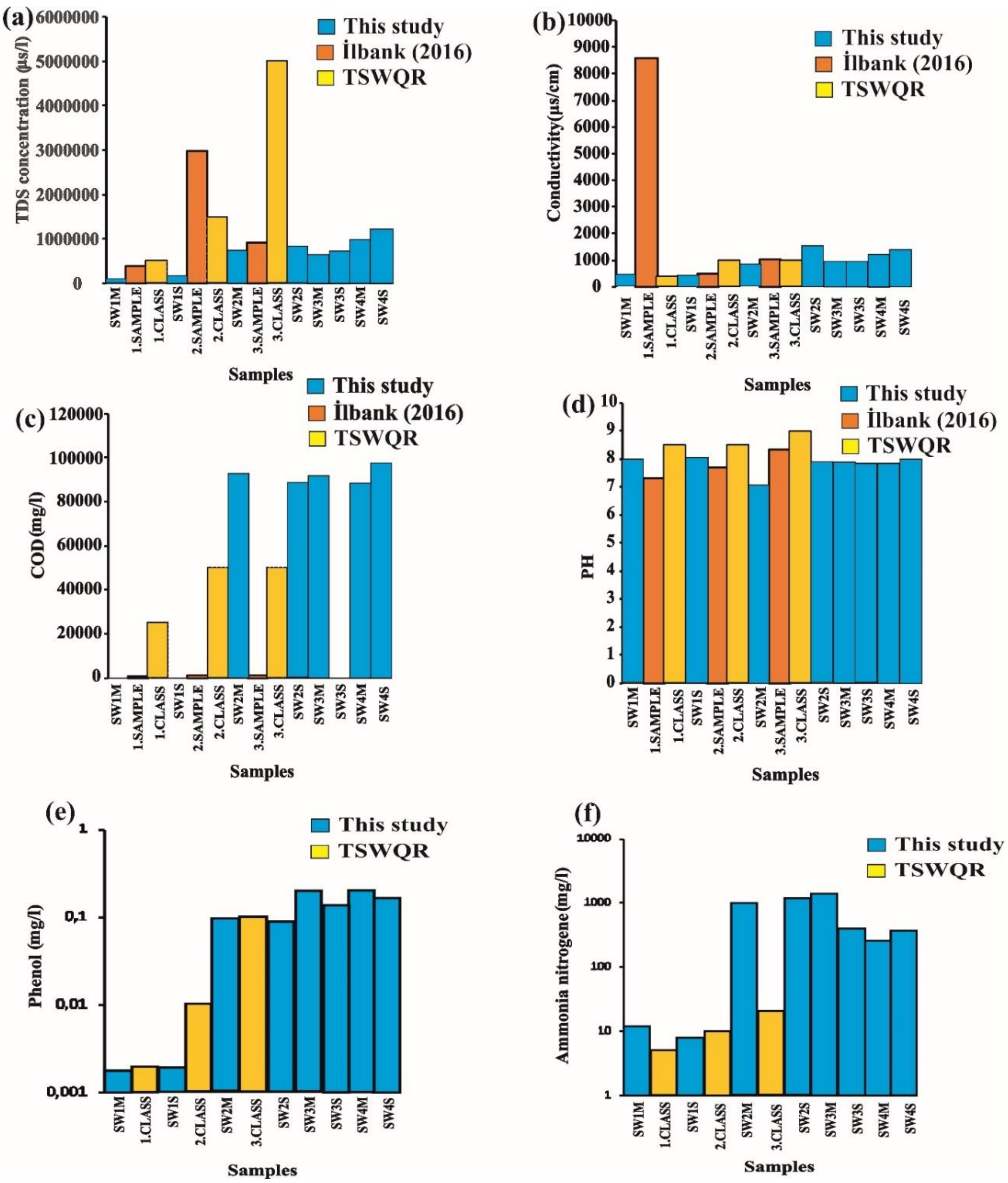

Figure 9. Histograms: this study, İlbank (2016) and TSWQR limits a) TDS concentration histograms, b) conductivity histograms, c) COD concentration histograms, d) pH test histograms, e) phenolic material concentration histograms f) ammonia nitrogen concentration histograms.

Table 3 Sub LPIs and overall LPI of the Eskişehir landfill drainage area waters (SW1-May)

Index	Parameters	Pollutant Conc	Sub-index value pi	Weight factor wi	wiPi
	COD	20.55	5	0.344444	1.72222
LPI organic	BOD	4.85	5	0.338888	1.69444
LPI_{or}	Phenolic compounds	0.0015	5	0.316666	1.58333
	LPI_{or}				4.999
	PH	7.99	3	0.214008	0.642023
	TKN	0.89	5	0.206226	1.031128
LPIinorganic	Ammonia nitrogen	12	5	0.198444	0.992218
LPI_{in}	TDS	100000	20	0.194553	3.891051
	Chlorides	58	5	0.18677	0.933852
	LPI_{inor}				7.4902
	Total chrominium	2,144	10	0,14128	1,412804
	Lead	0,163	6	0,139073	0,834437
	Mercury	0,002	5	0,136865	0,684327
Lis PI heavy	Arsenic	3,667	10	0,134658	1,346578
metals	Zinc	0,383	5	0,12362	0,618102
LPI_{hm}	Nickel	1,63	7	0,11479	0,803532
	Copper	0,001	5	0,110375	0,551876
	İron	231,67	10	0,099338	0,993377
	LPI_{hm}				7.245
Overall LPI		$0.232LPI_{or}+0.257LPIin+0.511LPI_{hm}$			6.78

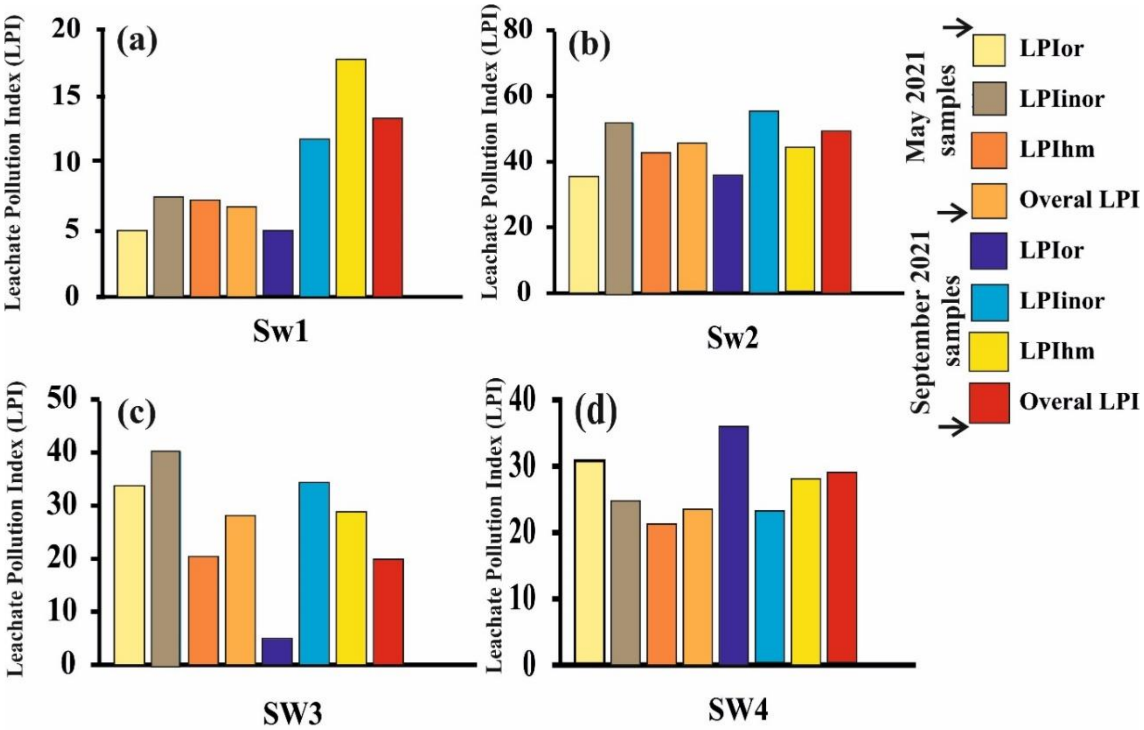

Figure 10. Histograms showing the LPI values: a) SW1 sample, b)SW2 sample, c)SW3 sample, d) SW4 sample.

Table 4 The LPI values determined in this study and the LPI values calculated according to the Turkiye Surface Water Quality Regulation (TSWQR 2021)

	SW1		SW2		SW3		SW4		TSWQR (2021)			
	May	Sept	May	Sept	May	Sept	May	Sept	1.class	2.class	3. Class	4.class
LPI_{or}	4.99	4.99	35.58	35.58	33.68	4.99	30.83	35.99	5.0	15.05	26,06	20.37
LPI_{inor}	7.49	11.809	51.77	55.33	40.23	34.35	27.74	23,27	5.0	5.0	7,04	7.04
LPI_{hm}	7.24	17.78	42.72	44.41	20.41	28.80	21.28	28.06	5.0	5.0	5.23	5.23
Overall LPI	6.78	13.28	43.39	45.17	28.58	24.70	24.64	24.65	5.0	7.4	9.20	9.20

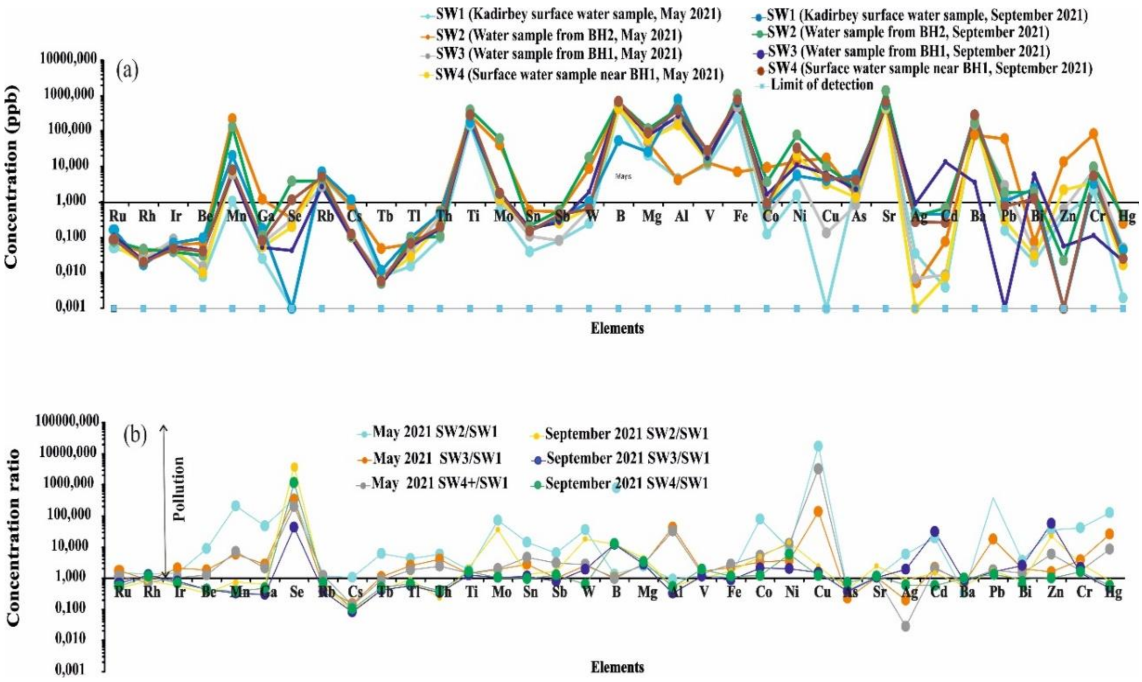

Figure 11. a) The trendline of heavy metal concentrations in water samples, b) the trendline of the ratio of heavy metal concentrations determined in water samples taken from the study area to the heavy metal concentrations in water samples taken from KFS.

Table 5 Correlation of quality criteria of water resources (TSWQR, 2021) and highest data determined at the study site.

Water quality parameters Inorganic pollution parameters (ppb)	Water classes I	 II	 III	 IV	Study site KFS	 Landfill drainage area
Hg	0.1	0.5	2	>2	0,046	0,051
Cd	5	5	10	>10	0,468	1,058
Pb	10	20	50	>50	1,063	6,189
As	20	50	100	>100	6.037	4.323
Cu	20	50	200	>200	4.169	17.53
Cr	20	50	200	>200	3.385	87.35
Co	10	20	200	>200	0.764	9.64
Ni	20	50	200	>200	5.67	147.36
Zn	200	500	2000	>2000	0.383	13.64
Fe	300	1000	5000	>5000	666,372	1118.79
Mn	100	500	3000	>3000	20.807	224.823
B	1000	1000	1000	>1000	55.338	725.04
Se	10	10	20	>20	0.001	3.981
Ba	1000	2000	2000	>2000	292.515	288.16
Al	300	300	1000	>1000	791.94	435.19

Table 6 Comparison of the heavy metal concentrations in water determined in this study with the limits of the World Health Organization (WHO, 2022).

WHO standarts 1996 (µg/l)		This study (µg/l)	
Metal	Limit	Lowest limit	Highest limit
Al	1170	149.982	435.019
Sb	4	0.085	0.580
As	12000	0.018	0.093
Ba	300	80.80	288.16
Be	1.2	0.01	0.071
Cd	3	0.008	1.07
Cr	50	2.144	9.883
Cu	2000	0.138	17.53
Fe	2000	505.02	1118.379
Pb	10	0.01	6.189
Mn	500	1.078	224.823
Hg	5	0.017	0.412
Mo	70	0.594	63.308
Ni	20	5.656	147.36
Se	10	0.200	3.981
Ag	100	0.001	0.415
Zn	3000	0.001	13.64

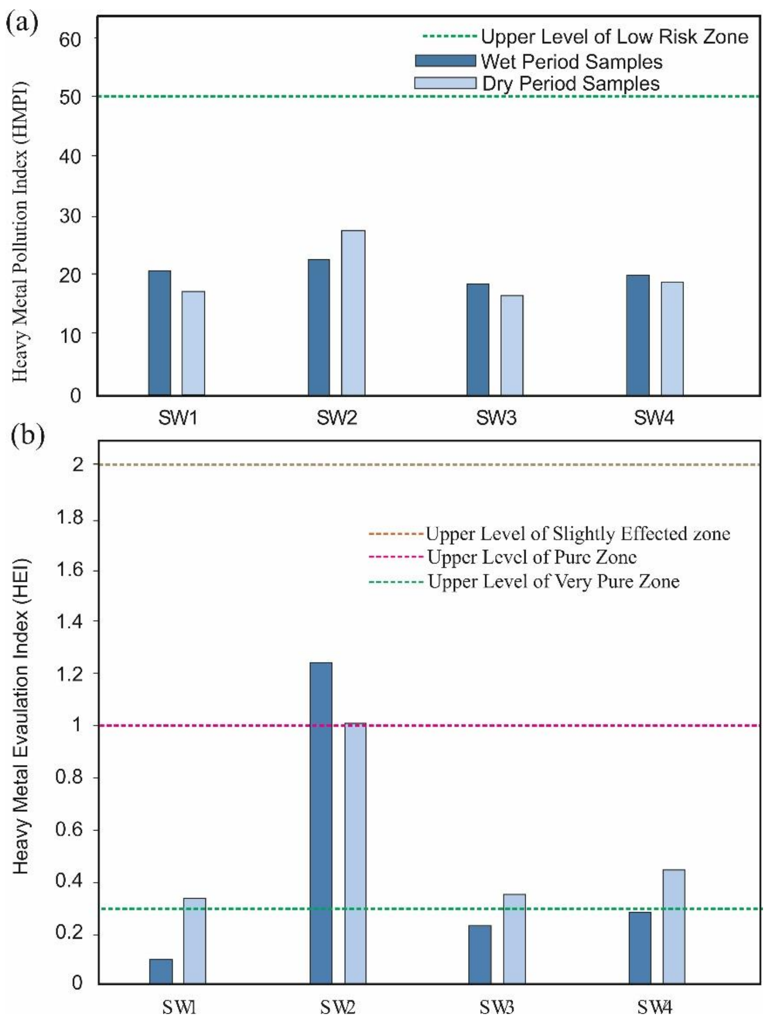

Figure 12. Pollution result histograms a) HMPI b) HEI

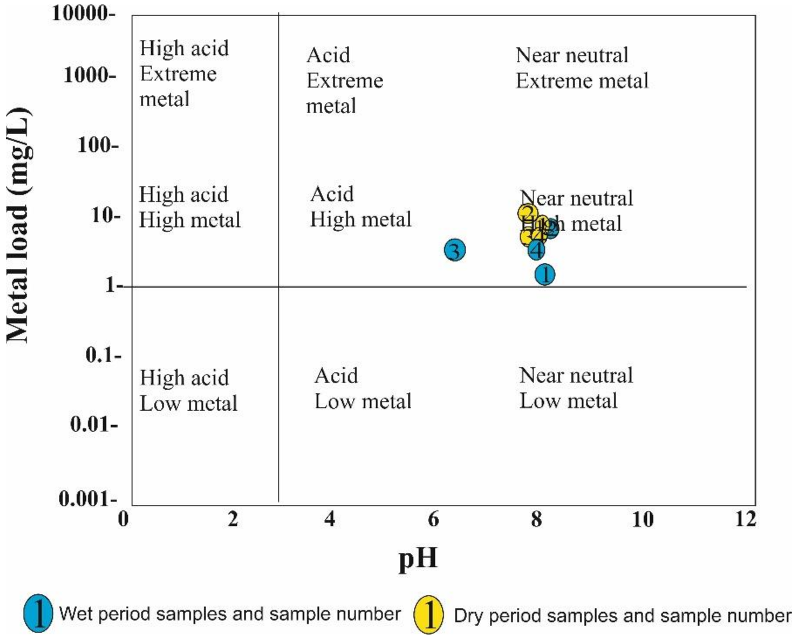

Figure 13. Water sample test results on diagram of metal load-pH chart.

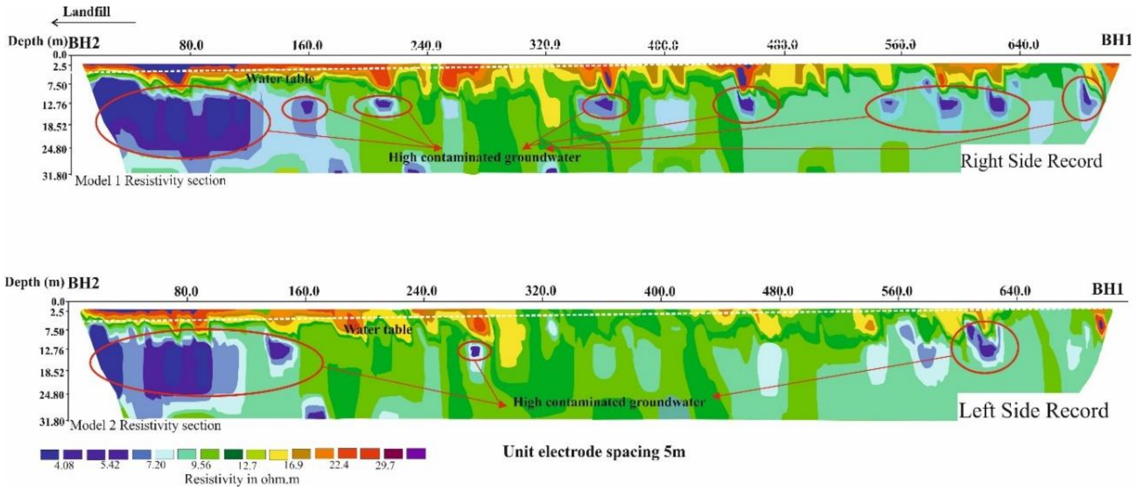

Figure 14. Right ant left side ERT measurements between BH2 and BH1.

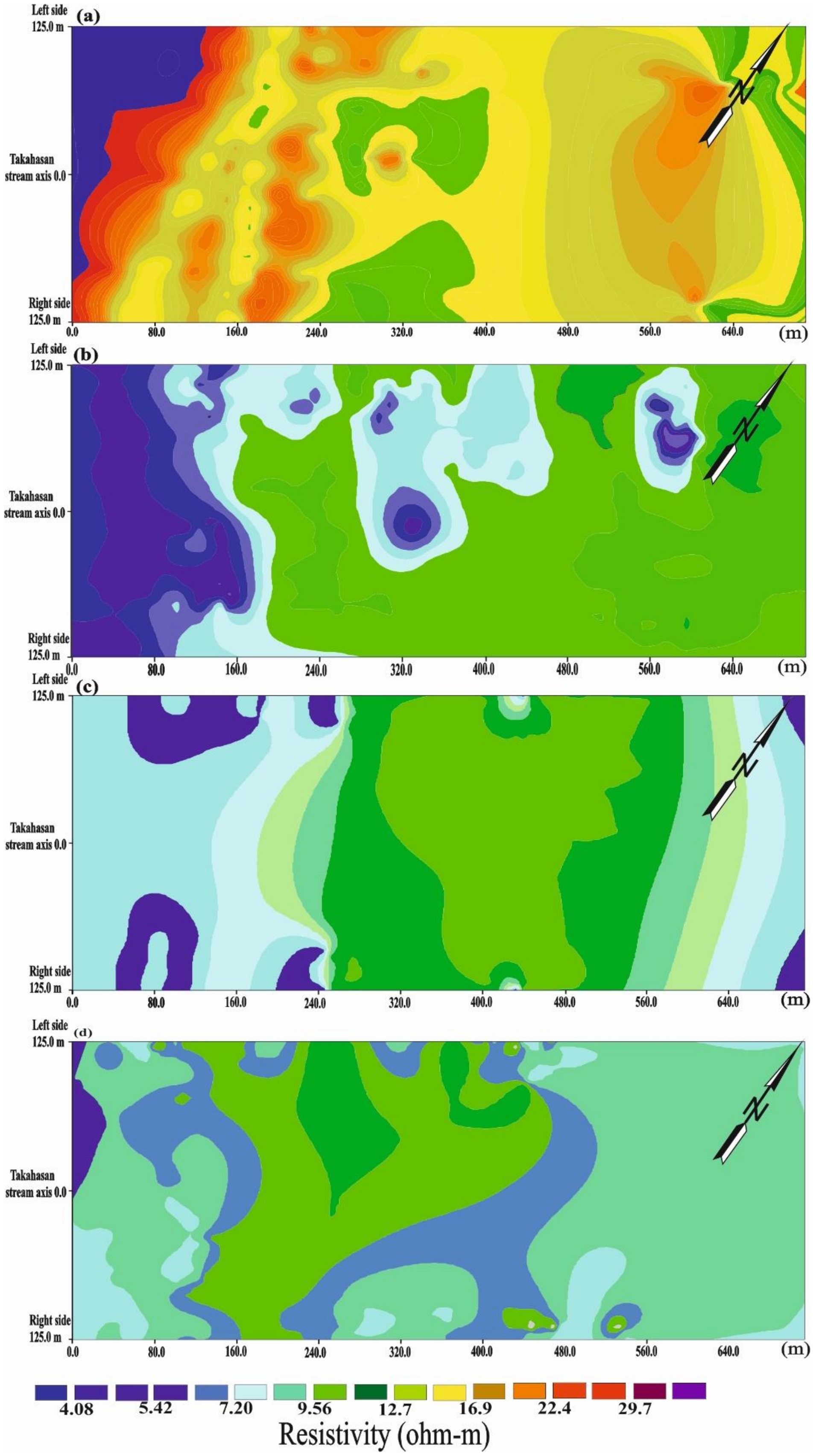

(a)
(b)
(c)
(d)
Left side
125.0 m
Takahasan
stream axis 0.0
Right side
125.0 m
0.0
80.0
160.0
240.0
320.0
400.0
480.0
560.0
640.0
(m)
N
4.08
5.42
7.20
9.56
12.7
16.9
22.4
29.7
Resistivity (ohm-m)

941

Figure 15. Resistivity maps for different depths rom ERT resistance measurements on the forehead 125 meters to the right and left of the Takahasan Stream, a) resistivity map at 2.5 m depth, b) resistivity map at 12.76 m depth c) resistivity map at 24.8 m deph, d) resistivity map at 31.8 m depth.

Appendix

Results of the heavy metal analysis on water samples

Heavy Metal (ppb)	Wet period (May 2021)				Dry period (September 2021)			
	SW1 (Kadirbey)	SW2 (SK2)	SW3 (SK1)	SW4 (Surface	SW1 (Kadirbey)	SW2 (SK2)	SW3 (SK1)	SW4 (Surface
Ru	0.052	0.079	0.091	0.061	0.168	0.079	0.117	0.092
Rh	0.029	0.038	0.025	0.021	0.017	0.047	0.025	0.021
Ir	0.042	0.062	0.090	0.045	0.070	0.04	0.057	0.049
Be	0.008	0.071	0.015	0.010	0.097	0.032	0.042	0.042
Mn	1.078	224.823	6.202	7.449	20.807	134.676	6.792	8.061
Ga	0.026	1.207	0.071	0.055	0.179	0.115	0.054	0.085
Se	0.001	0.353	0.336	0.200	0.001	3.981	0.043	1.174
Rb	5.316	6.551	2.694	6.542	7.159	4.074	2.767	5.242
Cs	0.744	0.776	0.111	0.103	1.182	0.106	0.098	0.125
Tb	0.008	0.005	0.005	0.006	0.012	0.005	0.005	0.006
Tl	0.016	0.068	0.041	0.029	0.103	0.094	0.059	0.069
Th	0.097	0.572	0.400	0.233	0.506	0.113	0.178	0.2
Ti	150.75	280.13	210.54	215.89	182.93	402.06	235.91	288.42
Mo	0.594	42.285	1.127	1.205	1.732	63.308	1.867	1.84
Sn	0.041	0.578	0.112	0.188	0.162	0.218	0.185	0.154
Sb	0.084	0.554	0.085	0.257	0.345	0.580	0.271	0.438
W	0.246	8.805	0.625	0.702	1.029	18.217	1.946	0.666
B	44.505	590.49	461.49	436.781	55.338	681.975	696.516	725.04
Mg	20.565	49.36	56.125	60.794	27.138	117.842	76.329	92.13
Al	46.350	430.2	198.09	149.982	791.994	435.019	266.330	407.86
V	11.209	13.38	18.931	15.349	15.217	15.215	17.550	28.80
Fe	231.67	728.0	505.02	639.407	666.372	1118.379	586.690	760.97
Co	0.123	9.64	0.423	0.653	0.764	3.74	1.652	0.93
Ni	1.63	147.36	6.144	20.970	5.656	80.015	11.557	33.89
Cu	0.001	17.53	0.138	3.208	4.169	9.98	6.482	4.94
As	3.667	1.55	0.845	1.354	6.037	2.601	2.331	4.323
Sr	444.43	497.88	468.48	468.64	570.245	1404.182	611.137	652.85
Ag	0.04	0.21	0.007	0.001	0.475	0.415	0.924	0.284
Cd	0.004	0.08	0.009	0.008	0.465	0.678	1.057	0.266
Ba	233.41	80.80	158.52	187.95	292.515	170.829	209.357	288.16
Pb	0.163	6.189	2.935	0.306	1.063	1.897	0.001	0.77
Bi	0.021	0.077	0.042	0.031	2.446	1.964	3.630	1.29
Zn	0.383	13.64	0.626	2.202	0.001	0.023	0.058	0.001
Cr	2.144	87.55	8.255	3.72	3.385	9.883	6.082	5.48
Hg	0.002	0.25	0.051	0.017	0.046	0.412	0.022	0.026